Rock Mechanics 15, 145—161 (1982)

Rock Mechanics
Felsmechanik
Mécanique des Roches

The Elasto-Visco-Plastic Analysis for Rock Displacement of the Foundation Pit of a Water Power Plant

By

Ge Xiu-run, Feng Ding-xiang, and Yang Jia-ling

With 16 Figures

(Received May 20, 1982)

Summary

The Elasto-Visco-Plastic Analysis for Rock Displacement of the Foundation Pit of a Water Power Plant. In this paper a method used in the elasto-visco-plastic analysis is proposed. It has been employed for deformation analysis of the foundation pit of a large water power plant in China.

The back analysis of this rock engineering problem shows that the relief of the rock initial stresses due to excavation and the rheological properties of the weak intercalations and the rock masses as well are the main factors which caused the large deformation of the foundation pit.

The results from the calculations are coincided fairly well with the data measured and observed in situ.

1. Introduction

A large Chinese hydro-electric station is under construction in a wide river valley of a hilly region. A river-run type power plant is located in the central portion of the river valley. The top opening of the foundation pit of the power plant is a square and its bottom is a rectangle, 279 m long and 28—45 m wide. The average depth of cut is 40—50 m and the upstream and downstream sides of the pit are cut into staged berms and other two sides into steep walls (Fig. 1) [1].

The azimuth of axis of the power-house is 109° (SE) or 289° (NW) and is nearly perpendicular to the strike of rock strata.

This region is composed of monocline in structure. The rock strata belong to the Lower Cretaceous series strata of land facies and have strikes of N 30° E, dips of SE and dip angles of 6°—8°. The rocks are chiefly argillaceous sillstones with little sandstones and ten more layers of weak intercalations. The profile of the cross section *A*—*A* in Fig. 1 is given in Fig. 2. The whole rock mass may be summarized as a bedded structure body of gentle and multiple bedding planes with numerous weak intercalations.

0035-7448/82/0015/0145/$ 03.40

After the foundation pit had been excavated to its initial configuration remarkable horizontal dislocations of the residual walls of presplit holes and the large bore holes were discovered along the weak intercalations and

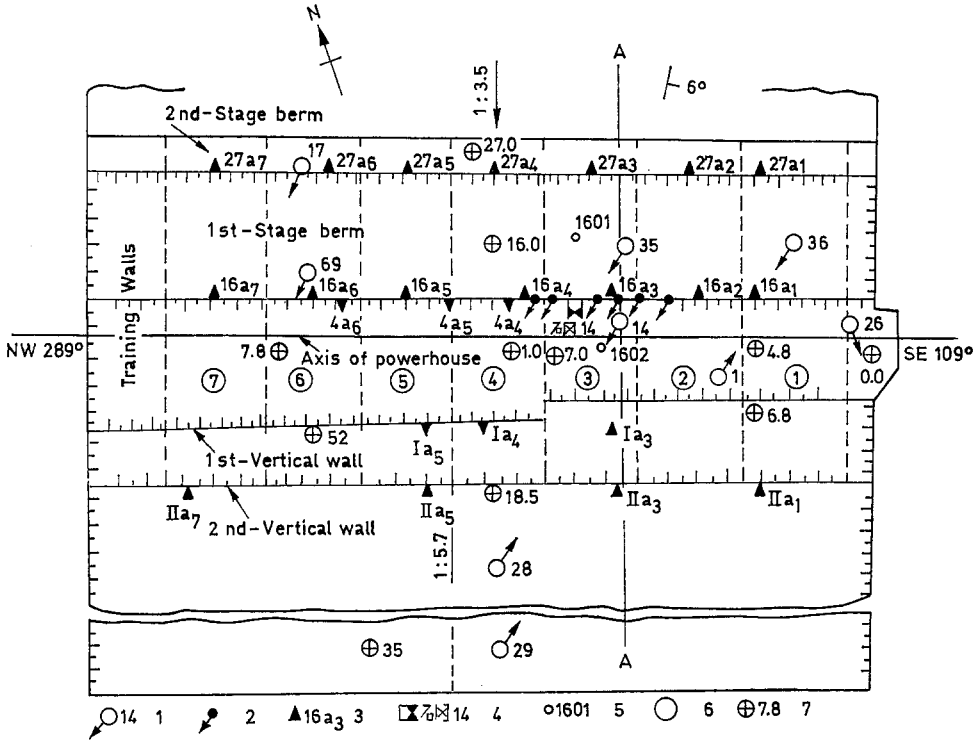

Fig. 1. Plans of observations for Rock-mass deformations (After Zeng et al. [1])

1. Bore holes (⌀ 1000 mm) and sequence number, arrowheads point to the directions of slip of intercalations.
2. Presplit drill holes and sequence number.
3. Observation points on the base-line and sequence number.
4. Observation galleries and sequence number.
5. Bore holes for measuring the geostress and sequence number.
6. Sequence number of units.
7. Elevations of excavated surface (m).

the maximum dislocations along the weak intercalation No. 212 is about 80 mm (Fig. 2). Hence more observations and studies were taken immediately.

The characteristics of the deformation observed in this foundation pit are as follows:

a) The horizontal deformations and dislocations have regularly specified directions and the axis of the power house is approximately a divide lines of the directions. The upstream rock masses moved in the directions of

206⁰—225⁰ azimuths (SW) and the downstream rock masses moved in 40⁰ azimuth (NE).

b) Horizontal dislocation, generally speaking, occurred along the weak intercalations, especially along four main weak intercalations, the numbers of which are 212, 202, 214 and 215.

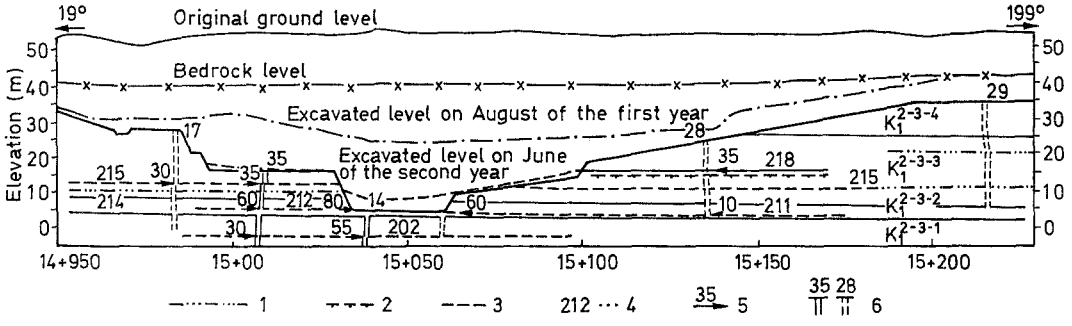

Fig. 2. Constructed profile showing dislocations of the rock masses along the weak intercalations (After Zeng et al. [1])

1. Argillaceous siltstone; 2. Psephitic claystone; 3. Claystone; 4. Notation for weak intercalations; 5. Direction of rock-mass dislocation and displacements; in mm; 6. Notation for ⌀ 1000 mm bore holes

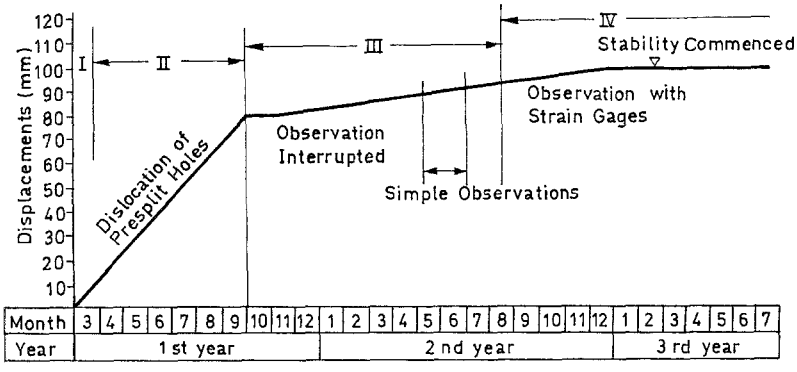

Fig. 3. Displacement curves of intercalation 212 (After Zeng et al. [1])

I. Presplit blasting; II. Foundation-pit excavation; III. Clearing and trimming of foundation; IV. After concrete placement

c) The deformations of the upstream and downstream sides of this rectangle pit are much larger than those occurring on the other two sides of the foundation pit.

d) After excavation the further development of the dislocations were measured for a long time. The horizontal displacement curves of weak intercalation No. 212 for more two years which is given in Fig. 3 show that rheological properties of rock masses of the foundation pit must be taken into account in analysis.

In combination with the data observed in situ a nonlinear finite element analysis, including the rheological analysis also, had been made in order to make a deformation calculation and to find out the main factors which caused the above mentioned remarkable horizontal dislocations.

The calculation shows that the relief of the residual geotectonic stresses preexisting in rock mass due to excavation and the rheological properties of the rock are the main factors which caused the large deformations of the foundation pit. The values of the initial stresses from the back analysis are coincided fairly well with the in situ measurements of stresses. And the calculated results of the deformations and dislocations considering the time effect of the rock are also good in compliance with the data measured and observed in situ for a long term.

The calculations were carried out on the electronic digital computer of Type DJS-8 with using the JR program designed by our institute.

2. Nonlinear Analysis

2.1 Models

Incremental procedure has been used here in the nonlinear analysis. When one of the principal stresses of triangle element used to represent rock in calculation has reached or exceeded the tensile strength of rock, the element is considered suffering tension failure, then the principal stress of it will be reduced much less than the original due to cracking. Therefore the strong anisotropic body must be considered in this case.

The Coulomb strength formula has been adopted here as a criterion of shear failure for rock. After suffering shear failure the stress state of the element will be determined according to the residual shear strength of the rock with assumption of keeping the first invariant of stress tensor as constant.

The joint element is employed to simulate the weak intercalations. The models of normal deformation, shear displacement deformation and shear strengths are given in Fig. 4 a, b, c. The tensile strength of joint element is $[\sigma_T]$. When $\sigma > [\sigma_T]$ the joint element not subjected to tension failure is considered to have tension failure occurring. When $V > \overline{V}$ or $V = \overline{V}$ and $dV > 0$, the opened out element will continue to maintain its open-out state, then $K_n = K_s = 0$ is adopted in this case. On the contrary reclosing of the opened out element occurs. The $V_{\max}$ in Fig. 4, *a* is used to describe the ultimate compaction state.

Three shear strength lines *B*, *C*, *A* in Fig. 4 c correspond to three characteristic points *B*, *C*, *A* in the shear displacement model in Fig. 4 b respectively.

The following expression is employed for describing the relationship between K_s and σ.

$$K_s = K_{s0} + \xi\sigma \tag{1}$$

where K_{s0} and ξ can be determined according to the experimental data.

If the sheared off joint element is still in the state of loading and continuous to have shear sliding, we treat the problem with considering the flow rule of a perfect plastic body. The details of the nonlinear analysis method for joint element can be found in references [2] and [3].

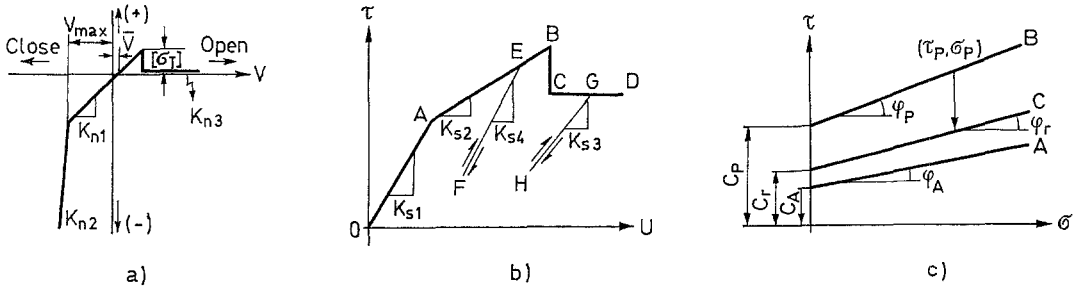

Fig. 4. The mechanical non-linear properties of weaknessplanes
(a) Normal deformation model; (b) Shear displacement model; (c) Shear strength lines

2.2 Conditions for Calculation

According to the plane strain condition and the profile given in Fig. 2 for the finite element analysis of this problem, we use the mesh shown in Fig. 5 in which the weak intercalations have been simplified as the three lines corresponding to the 202, 212, 215 intercalations respectively.

Before excavation of foundation pit the total numbers of nodes, triangles and joint elements are equal to 386, 478 and 121. After excavation the total numbers reduced to 337, 381 and 110 correspondingly.

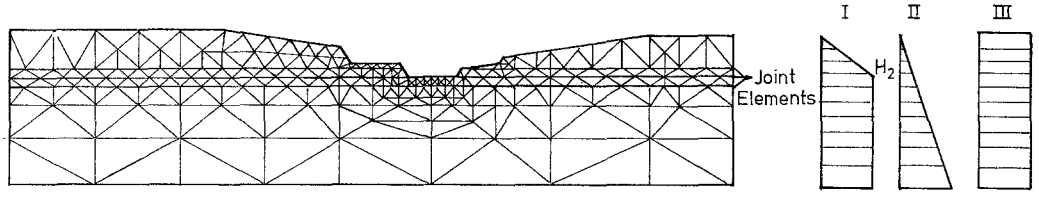

Fig. 5. The mesh for calculation and three types of distribution of σ_x

The unloading procedure due to excavation of the pit was realized in calculation by three stages according to the practical situation in situ.

We have made some assumptions for describing the initial stress state of rock mass of the foundation pit before excavation, i. e. $\sigma_y = -\gamma H$ and $\tau_{xy} = 0$. But what about the σ_x is not clear. So three types of distribution of σ_x have been taken into account and can be found in Fig. 5. The H_2 is used as a characteristic value representing the horizontal stress at the level of the bottom of the pit. Three different values such as $H_2 = -20$ kg/cm^2, $H_2 = -22$ kg/cm^2 and $H_2 = -25$ kg/cm^2 have been taken in calculation. The *I*

type of distribution of σ_x for $H_2 = -22$ kg/cm^2 is the basic scheme, its calculation results are best in compliance with the practically measured data of deformation in situ.

According to the tests in situ the mechanical parameters of rock are as follows: $E = 16000$ kg/cm^2, $\nu = 0.3$ and $\gamma = 2.4$ t/m^3, $C = 7$ kg/cm^2 and tan $\varphi = 1.26$ for the peak shear strength, and $C = 2.3$ kg/cm^2, tan $\varphi = 0.9$ for the residual shear strength.

Table 1. *The Main Mechanical Properties of Weak Intercalations*

Intercalations No.	Shear strength C (kg/cm^2)	tan φ	Residual shear strength C (kg/cm^2)	tan φ	$[\sigma_T]$ (kg/cm^2)	K_{n1} (kg/cm^3)	K_{s0}	ξ
202 212 211	0.32	0.204	0.32	0.204	0	98	2	6
215	0.32	0.3	0.32	0.3	0	196	4	12

The main mechanical properties of weak intercalations No. 202, 212 and 215 obtained from large scale tests in situ are given in Table 1.

2.3 Some Results of Nonlinear Analysis

The dislocations along the weak intercalations at the points *A*, *B*, *C*, *D*, *E*, *F*, *G* (Fig. 6) observed and measured when the excavation of the pit was just finished can be found in Table 2, and the calculated dislocations at

Table 2. *List of the Calculated Dislocations and the Measured Dislocations Along the Weak Intercalations* (mm)

Location	A	B	C	D	E	F	G
Calculated dislocation	20.5	35.0	61.9	85.5	84.0	12.9	28.0
Measured dislocation	30	35	60	80	60	35	10

these points are listed here in the same Table. The points *B*, *C*, *D* are located in the large holes on the profile of *A*—*A*, while the points *A*, *E*, *F*, *G* are projections of the points in the bore holes on near *A*—*A*.

The distributions of stresses and displacements in the parts *JD* and *EG* of weak intercalations shown in Fig. 6 are given in Fig. 7 and Fig. 8 respectively.

In order to check and demonstrate the existence, direction and amount of the residual geostresses of rock the stress measurement has been done in situ, and three boreholes have been especially set up for the stress relief method [4]. Two boreholes of them were located in the area of the foundation pit of the water power plant. The another one was located at a place 500 meters downstream of the foundation pit beyond the influence sphere of excavation.

For every borehole from the groundsurface to the depth of the 40 m the stress measurements were carried out at 8—10 points. The principle of the used method is based on the measuring the deformations of the borehole

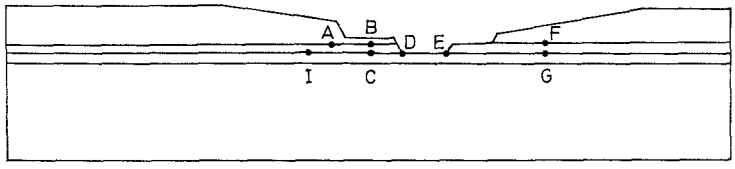

Fig. 6. Locations of some characteristic points

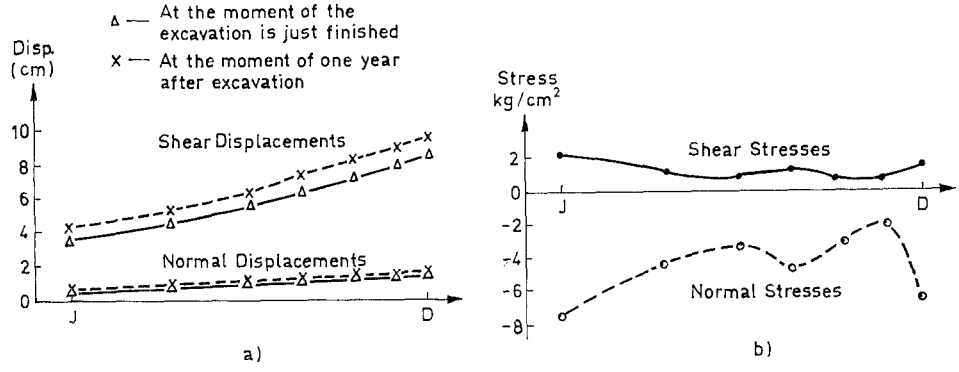

Fig. 7. The distributions of displacements and stresses in the part J D of weak intercalation (a) Relative displacements; (b) Stresses

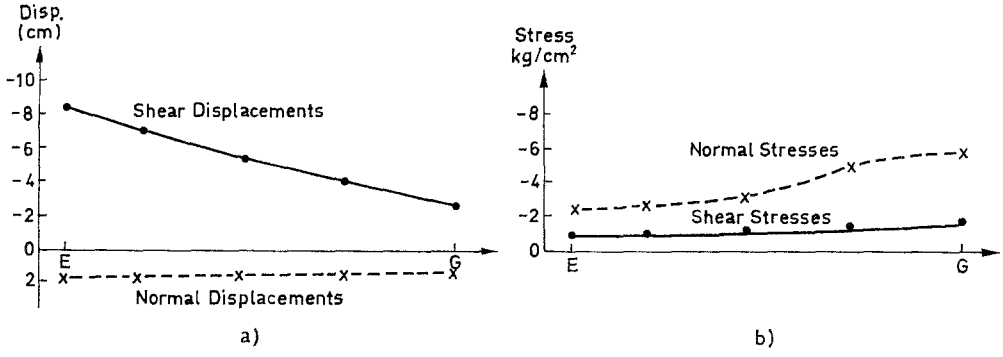

Fig. 8. The distributions of displacements and stresses in the part E G of weak intercalation (a) Relative displacements; (b) Stresses

by means of the overcoring technique (Fig. 9). The special equipment for measuring the deformations of the wall of the small borehole has the diameter of 36 mm. In this equipment there are four deformation transducers by means of which we can measure the deformations along four different directions of diameter simultaneously. The used transducer consists of a thin

steel ring with four strain gages. The diameter of the overcoring borehole is about 130 mm. From the Young's modulus and the measured data of the deformations of the small borehole after the overcoring process the rock stresses on the plane which is perpendicular to the axis of the borehole can be calculated.

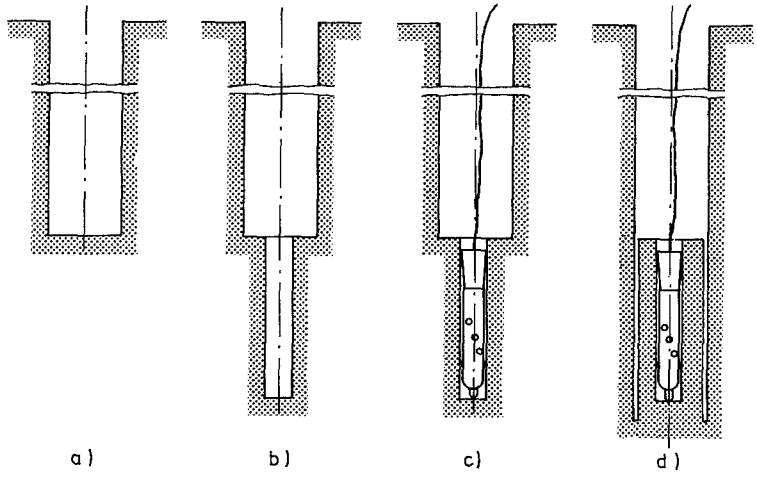

Fig. 9. The sketch of the overcoring technique

The stress measurement in situ has proved up the existing of the residual geotectonic stresses of rock in the region of the foundation pit. Results proved that the directions of maximum principal compressive stresses on the horizontal plane were N 30^0—50^0 E and were basically in coincidence with the directions of principal compressive stresses of the recent structure of the region as well as the directions of the rock mass displacement of the foundation pit. The distributions of the measured stresses in situ along the borehole are shown in Fig. 10 [4].

According to the measured data in situ the values of the horizontal stresses at level of the bottom before the excavation are: $\sigma_1 = -31$ kg/cm^2, $\sigma_2 = -23$ kg/cm^2, and the direction of the σ_1 is about N 30^0 E.

Considering that there are some simplifications used in the calculation, the calculated result of horizontal initial stress from the back analysis, i. e. about -22 kg/cm^2 is fairly well in compliance with the measured data. The details of the calculation can be found in reference [5].

The results obtained from linear or nonlinear analysis for this engineering problem under the same conditions are quite different. For linear case the calculated horizontal dislocation, for example, at the point D is about 5 mm, but it is 85.8 mm for nonlinear analysis at the same point.

Besides, we have also done the nonlinear analysis based on the assumption of that the initial horizontal stresses are only caused and can be calculated by gravity. In respect of this case the calculated horizontal disloca-

tion at point D would not be more than 1 mm. So it is no doubt that only the gravity couldn't cause such large dislocations after excavation due to unloading. It is also proved up by the calculation that, apart from the existing

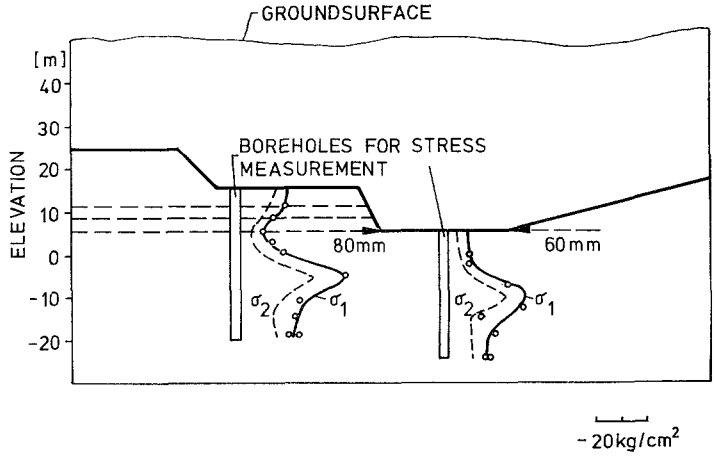

Fig. 10. The distribution of the Geostresses σ_1 and σ_2

of residual stresses of rock the continuous spreading of weak intercalations in the region near the surface of rock slope is an important condition for occurring of such large dislocations of the foundation pit.

3. The Analysis of Rheological Properties of Rock Masses

After excavation of the pit horizontal deformations along the weak intercalations still developed. It is necessary to make the analysis of creep problem.

3.1 Method of Analysis

3.1.1. The whole time T for which we have to analyse the creep problem is divided into a sequence of intervals.

The elasto-plastic analysis was carried out for the situation when the foundation pit had just been excavated. Afterwards in order to consider the time effect it was assumed that the stress state of the element will maintain constant for each time interval before adjustment has been adopted, hence based on the stress state of the beginning of the interval and the rheological deformation curve of shearing of weak intercalation the increase of relative displacements or strain can be found out. Then the new stress and strain state at the end of the interval of the time will be worked out.

3.1.2. The rheological behaviour of joint and weak intercalations and its simplification.

The rheological shear-displacement curves of the weak intercalations of argillaceous siltstone obtained from the large scale rheological tests in situ are shown in Fig. 11 [6].

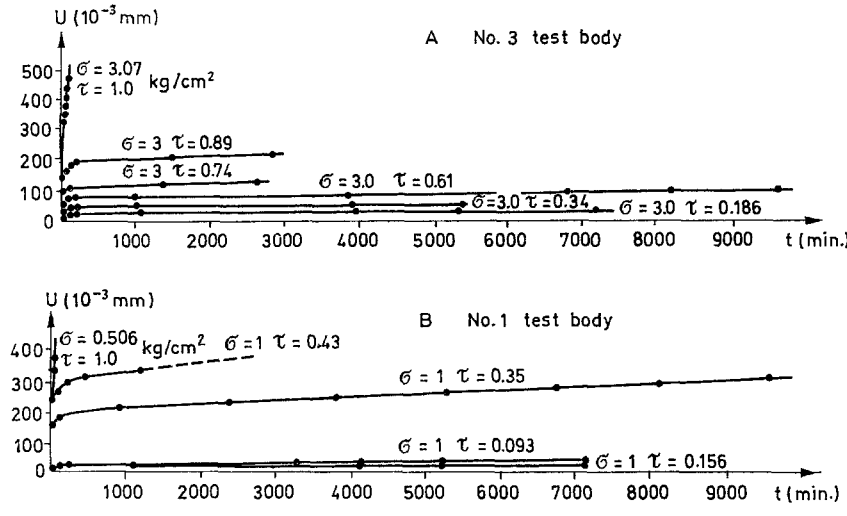

Fig. 11. The rheological shear-displacement curves

The time effect cannot be neglected, when the following condition has been fulfilled.

$$|\tau| > \tau_A = |\sigma| \tan \varphi_A + C_A, \quad \text{when } \sigma < 0. \tag{2}$$

The value of relative shear displacement due to the rheological property depends upon the dimensionless parameter S.

$$S = \frac{|\tau| - |\tau_A|}{|\tau_A|} \tag{3}$$

and $S=0$, when $|\tau| < |\tau_A|$.

The function of relative shear displacement versus time under condition $S=1$ is written as $\bar{u}(t)$, then the corresponding rate of displacement versus time is $\bar{\varphi}(t)$

$$\bar{\varphi} = \frac{d\bar{u}}{dt}. \tag{4}$$

The further simplification is that the $u(t)$ and $\varphi(t)$ in any stress state can be calculated with the following formula

$$\begin{aligned} u(t) &= \bar{u}(t) \cdot S \\ \varphi(t) &= \bar{\varphi}(t) \cdot S \end{aligned} \tag{5}$$

The whole time T is divided into intervals ($T = \sum_{i=1}^{n} \Delta t_i$). Hence $t_0 = 0$, $t_1 = \Delta t_1$, $t_i = t_{i-1} + \Delta t_i$ $(i = 2, 3, \ldots)$ and $t_n = T$.

The relative shear displacement of joint element due to creep at the time interval Δt_i is noted by Δu^c.

If the external load is not changed during the term of T, and the adjustment of stress is not large, the following equation can be used approximately

$$\Delta u^c = \left(\frac{\bar{\varphi}(t_{i-1}) + \bar{\varphi}(t_i)}{2}\right) \cdot S(t_{i-1}) \cdot \Delta t_i. \tag{6}$$

The equivalent nodal forces of the joint element $\{\Delta F\}_c$ might be easily calculated from Δu^c. Then the $\{\Delta R\}$ can be obtained, and corresponding adjustment of the stresses can be made.

For interval Δt_i following equation should be solved

$$[K]\{\Delta\delta\}^c = \{\Delta R\}. \tag{7}$$

The increments of the stresses at the interval Δt_i marked as $\{\Delta\sigma\}_{\Delta t_i}$ can be worked out from $\{\Delta\delta\}^c$. Then the stresses and displacements at the time $t = t_i$ may be claculated by

$$\begin{aligned} \{\sigma\}_{t=t_i} &= \{\sigma\}_{t=t_{i-1}} + \{\Delta\sigma\}_{\Delta t_i} \\ \{\delta\}_{t=t_i} &= \{\delta\}_{t=t_{i-1}} + \{\Delta\delta\}_{\Delta t_i} \end{aligned} \tag{8}$$

The rheological behaviour of the weak intercalation can be represented by the model shown in Fig. 12, in which H, P_i and N_i are the symbols of the elastic, plastic and viscous elements respectively.

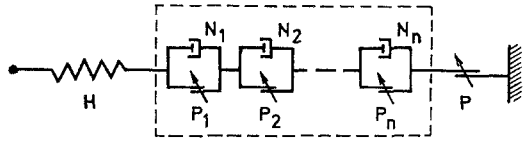

Fig. 12. The rheological model

At the moment of loading ($t = 0$) the elements within the block marked by dashed line in Fig. 12 act as the rigid body, hence the analysis is just like for the elasto-plastic body. With the increase of the loading time and due to the existing of viscous elements, the flow may occur. Because the viscous elements are in parallel connection with the plastic elements, for which the Coulomb formula is used as criterion P_i in form of S ($P_n > P_{n-1} > \ldots > P_2 > P_1$) therefore the rheological deformation will not be appearing if $S < P_1$. When $S > P_1$, and S is increasing gradually the plastic elements are sliding one after another, then the rate of rheological displacement is increasing with the rise of S.

The adjustment has been made by using the equivalent nodal forces. Since during the adjustment the elements within the block marked by the dashed lines can be considered as rigid bodies again, the elasto-plastic analysis can be used here.

3.1.3. A method of calculating the deformation due to rheology in consideration of stress history.

The equation for calculating the relative shear displacement of joint element due to creep at the moment t is as follows

$$u^c(t) = \int_0^t S(\theta)\, \bar{\varphi}(t-\theta)\, d\theta. \tag{9}$$

The symbols used here are refered to the Fig. 13. It can be also approximately written in the following form

$$u^c(t_m) = \sum_{i=1}^{m} S(\theta_i')\, \bar{\varphi}(t_i^m)\, \Delta\theta_i \tag{10}$$

where $t_i^m = t_m - \theta_i'$.

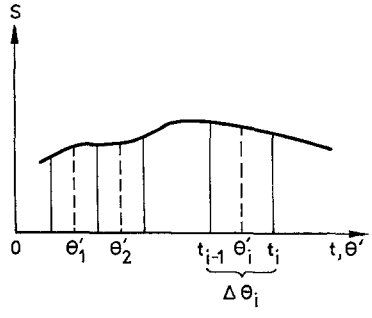

Fig. 13. The sketch of time intervals during considering the stress history

Therefore the relative shear displacement due to rheology at the interval $\Delta\theta_m$ can be calculated

$$\Delta u^c(\Delta\theta_m) = S(\theta_m')\, \bar{\varphi}(t_m^m)\, \Delta\theta_m + \sum_{i=1}^{m-1} S(\theta_i')\, \Delta\bar{\varphi}(t_i^m)\, \Delta\theta_i \tag{11}$$

where

$$\Delta\bar{\varphi}(t_i^m) = \bar{\varphi}(t_i^m) - \bar{\varphi}(t_i^{m-1}). \tag{12}$$

When the changes of S are not large following simplification has been employed effectively in this paper

$$\Delta u^c(\Delta\theta_m) = S(\theta_m')\, \bar{\varphi}(t_m^m)\, \Delta\theta_m + S(\theta_{m-1}')\, \Delta\bar{\varphi}(t_{m-1}^m)\, \Delta\theta_{m-1} + \\ + S(\theta_{m-2}')\, \Delta\bar{\varphi}(t_{m-2}^m)\, \Delta\theta_{m-2} + S(\theta_{m-3}') \sum_{i=1}^{m-3} \Delta\bar{\varphi}(t_i^m)\, \Delta\theta_i \tag{13}$$

3.1.4 The rheological analysis of rock element.

The method can be found in reference [7].

$$\dot{\varepsilon}_{ij}^c = \frac{3}{2} \frac{\dot{\varepsilon}_e^c}{\sigma_e} S_{ij} \tag{14}$$

where

$$S_{ij} = \sigma_{ij} - \frac{1}{3}\delta_{ij}\sigma_{kk}. \tag{15}$$

The increments of strains in consideration of time effect at the interval for plane-strain problem are as follows

$$\begin{aligned}
\Delta\varepsilon_x^c &= \frac{\dot{\varepsilon}_e^c}{\sigma_e}\left(\sigma_x - \frac{1}{2}(\sigma_y+\sigma_z)\right)\cdot\Delta t \\
\Delta\varepsilon_y^c &= \frac{\dot{\varepsilon}_e^c}{\sigma_e}\left(\sigma_y - \frac{1}{2}(\sigma_z+\sigma_x)\right)\cdot\Delta t \\
\Delta\varepsilon_z^c &= \frac{\dot{\varepsilon}_e^c}{\sigma_e}\left(\sigma_z - \frac{1}{2}(\sigma_x+\sigma_y)\right)\cdot\Delta t \\
\Delta\varepsilon_{xy}^c &= \frac{3}{2}\frac{\dot{\varepsilon}_e^c}{\sigma_e}\tau_{xy}\cdot\Delta t.
\end{aligned} \tag{16}$$

The $\frac{\dot{\varepsilon}_e^c}{\sigma_e}$ represents the rheological behaviour. It can be obtained from axial tests of rheology. At that time, $\sigma_c=\sigma_1$, $\dot{\varepsilon}_e^c=\dot{\varepsilon}_1^c$.

3.2 Conditions for Calculation Considering the Time Effect

For calculation of rheology the term of one year after the excavation of the foundation pit is divided into 21 intervals. The total term of the first 10 intervals lasts one month and each of them is in turn equal to 0.083, 0.083, 0.124, 0.25, 0.46, 1.0, 2.0, 3.0, 7.0, 16.0 days. Each of the rest 11 intervals is equal to 1 month.

It is appropriate to assume that the rheological deformation of the foundation pit after excavation is caused by the stresses due to unloading, i. e. the difference between the current and the initial stress state of rock masses of the foundation pit.

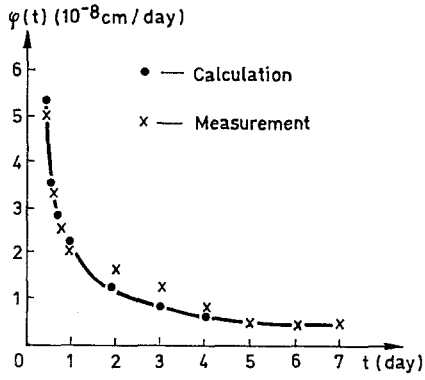

Fig. 14. $\bar{\varphi}(t)$ function curve

In accordance with the measured curves obtained from the rheological shear tests in situ the following expression can be used approximately to represent $\bar{\varphi}(t)$ (Fig. 14)

$$\bar{\varphi}(t) = (0.34\, t^{-2.1} + 1.774\, t^{-1.307} + 7.25\, t^{-0.662})/486 \tag{17}$$

where $\bar{\varphi}(t)$ ... cm/day, t ... day.

Because of lack of the measured data after 7 days, some different assumptions are used for $\bar{\varphi}(t)$.

Considering lack of the experimental data from the large scale tests in situ about the rheological parameters of rock, $\frac{3}{2}\frac{\dot{\varepsilon}_e^c}{\sigma_e} = 2.5 \times 10^{-7}$ cm²/kg·day is accepted in calculation in accordance with the observations of deformation during long time after excavation and this parameter is approximately equal to the value obtained from laboratory tests of the rock.

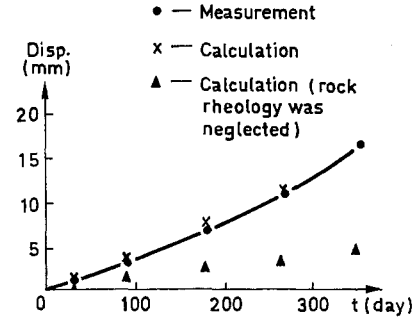

Fig. 15. Rheological displacement curve at the point D of weak intercalation

3.3 Results of Calculation for Creep Problem

The dislocations at the point *D* (Fig. 6) due to rheological properties of rock for one year after excavation are calculated and given in Table 3. They are in good coincidence with the observation in situ. It can be seen in Fig. 15.

Table 3. *The Rheological Dislocations Along the Weak Intercalation at the Point D*

Rheological time (day)	1	7	14	30	90	180	270	360
Rheological disloc. (cm)	0.04	0.07	0.09	0.14	0.33	0.71	1.15	1.63

The deformations of the foundation pit at the moment when the pit had just been excavated and at the moment of the tenth month's end after excavation are illustrated in Fig. 16.

The dislocations at the portion *JD* of the weak intercalation (Fig. 6) at the moment of one year after excavation are also shown in Fig. 7.

3.4 Discussion

A lot of examples under different conditions have been also calculated in order to investigate the influence of the selection of different methods of the treatment and rheological parameters. The conditions of calculation for

some of these examples and corresponding dislocations at the point D are given in Table 4.

Table 4. *Some Examples of Rheological Calculation and Their Calculated Rheological Dislocations Along the Weak Intercalation at the Point D*

No. of example	Rhèological parameter of rock $\frac{3}{2}\frac{\dot{\varepsilon}_e^c}{\sigma_e}$ $cm^2/kg \cdot day$	Rheological timef(day) and rheological dislocations (cm)							
		1	7	14	30	90	180	270	360
21*	0	0.04	0.05	0.06	0.09	0.17	0.28	0.37	0.45
+22*	2.5×10^{-7}	0.04	0.07	0.09	0.14	0.33	0,71	1.15	1.63
24*	1.0×10^{-7}	0.04	0.06	0.07	0.11	0.24	0.48	0.75	0.85
25**	0	0.01	0.02	0.02	0.04	0.13	0.24	0.34	0.43

+ The basic scheme.
* The rheological behaviour of weak intercalations was calculated according to 3.1.2.
** The rheological behaviour of weak intercalations was calculated according to 3.1.3.

From these examples some things are clear:

a) Generally speaking, the rheological behaviour of the weak intercalations is much more obvious than that of the rock. But it does not mean that the rheological properties of the rock can be neglected when dealing

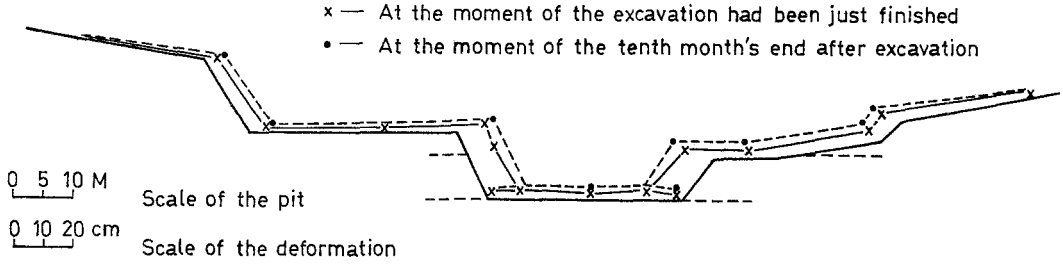

Fig. 16. The displacements of the surface of the foundation pit obtained from calculation

with the rock engineering problem. The dislocation occurring at the point D not only depends upon the behaviour of weak intercalation but also the rheological behaviour of rock of the whole region (Fig. 15).

b) The rheological parameter of rock gives the large influence on the dislocations of weak intercalations of the foundation pit.

c) Two methods for estimating the rheological deformation of joint element including the method in consideration of the stress history are quite different, but because the changes of stresses are not serious the differences between the results given by them are rather small.

4. Conclusions

a) A method practically used in the elasto-visco-plastic analysis is proposed in this paper. It has been employed for deformation analysis of the foundation pit of a large hydro-electric station in consideration of rheological properties of rock and weak intercalation.

b) A back analysis of a rock engineering problem based on the some data measured and observed in situ in accordance with the particular conditions, generally speaking, is often helpful to gain an insight into this problem and get some useful informations and results.

c) For this large hydro-electric power station the horizontal initial stress of rock at the elevation of the bottom of the pit before excavation is about $-22\ kg/cm^2$ obtained from the back analysis. It agrees fairly well with the geostress measurement in situ.

d) Apart from the existing of residual stresses of rock the continuous spreading of weak intercalation in the region near the surface of rock slope is an important condition for occurring of such large dislocations of the foundation pit.

e) In many cases, even if the rock is soft, the strata are nearly horizontal, but the existence and influence of initial stresses in rock (residual geotectonic stress) often seem to be an important factor which should be taken into account in rock engineering problem.

f) The dislocations of weak intercalation for a long term not only depend upon the rheological properties of itself, but also the rheological properties of rock. In this example the calculated dislocation of weak intercalation in consideration of only the rheological properties of weak intercalation itself is merely about $1/4$ of the observed data in situ.

g) Both methods introduced in this paper for calculating the rheological displacement of joint element including the stress history give rather similar results if the external loads are not changed and the changes of stress state during the whole process are not serious.

h) The relief of the initial stresses of rock due to excavation and the rheological properties of the rock masses and weak intercalations are the main factors which caused the large deformation of the foundation pit of the hydro power plant.

References

[1] Zeng Chao-min, Chou Hsing-chih, Hsu Jui-chun: Rock-mass Deformations in Gentle and Multiple Weakly-intercalated Bedrocks During Deep Excavation of the Foundation Pit. (This paper was introduced in the 3rd International Conference on Engineering Geology, Madrid, September, 1978).

[2] Ke Hsu-jun (Ge Xiu-run): Non-linear Analysis of the Mechanical Properties of Joint and Weak Intercalation in Rock. Proceedings of the 3rd International Conference on Numerical Methods in Geomechanics, Vol. 2, Aachen, April 2—6, 1979.

[3] Ge Xiu-run: Non-linear Analysis of Joint Element and Its Application in Rock Engineering. Int. J. of Num. and Analyt. Methods in Geomechanics 5, 229—245 (1981).

[4] Li Guang-yu, Bai Shi-wei: In-Situ Study on Stress in Rock Mass, Journal of Rock and Soil Mechanics, Institute of Rock and Soil Mechanics, Academia Sinica, Wuhan, China, No. 1, 76—90, 1979.

[5] Feng Ding-xiang, Yang Tia-ling, Ge Xiu-run: Finite Element Analysis for Rock Displacement of Foundation Pit of a Water Power Plant. Chinese Journal of Geotechnical Engineering 2, 43—54 (1980).

[6] Xu Dong-jun: The Rheological Behaviour of the Weak Rock Mass and the Method of Determining Long-Term Strength, Journal of Rock and Soil Mechanics, Institute of Rock and Soil Mechanics, Academia Sinica, Wuhan, China, No. 1. 37—50, 1980.

[7] Klein, J.: The Application of Finite Elements to Creep Problems in Ground Freezing, Proceedings of the 3rd International Conference on Numerical Methods in Geomechanics, Vol. 1, Aachen, April 2—6, 1979.

Address of the authors: Ge Xiu-run, Feng Ding-xiang, and Yang Jia-ling, Institute of Rock and Soil Mechanics, Academia Sinica, Wuhan, China. Ge Xiu-run, Research Fellow of the Alexander von Humboldt-Stiftung, Institut für Bodenmechanik und Felsmechanik der Universität Karlsruhe, Richard-Willstätter-Allee, D-7500 Karlsruhe, Federal Republic of Germany.